HAL
archives-ouvertes.fr

High precision position measurements at high counting rates with drift chambers and multi-hit electronics

M. Mac Cormick, W. Mittig, P. Roussel-Chomaz, M.D. Cortina-Gil, C. Spitaels, J.F. Libin, J.M. Casandjian, M. Chartier, F. Auger, S. Ottini, et al.

▶ **To cite this version:**

M. Mac Cormick, W. Mittig, P. Roussel-Chomaz, M.D. Cortina-Gil, C. Spitaels, et al.. High precision position measurements at high counting rates with drift chambers and multi-hit electronics. 1998, pp.1-11. <in2p3-00566499>

HAL Id: in2p3-00566499
http://hal.in2p3.fr/in2p3-00566499

Submitted on 16 Feb 2011

HAL is a multi-disciplinary open access archive for the deposit and dissemination of scientific research documents, whether they are published or not. The documents may come from teaching and research institutions in France or abroad, or from public or private research centers.

L'archive ouverte pluridisciplinaire **HAL**, est destinée au dépôt et à la diffusion de documents scientifiques de niveau recherche, publiés ou non, émanant des établissements d'enseignement et de recherche français ou étrangers, des laboratoires publics ou privés.

GRAND ACCELERATEUR NATIONAL D'IONS LOURDS

GANIL

High Precision Position Measurements at High Counting Rates with Drift Chambers and Multi-hit Electronics

GANIL R 98 02

Laboratoire commun CEA / DSM - CNRS / IN^2P^3

B.P. N° 55027 - 14076 CAEN CEDEX 5 - TÉL. 02.31.45.46.47 - TÉLÉCOPIEUR 02.31.45.46.65
GROUPEMENT D'INTÉRÊT ÉCONOMIQUE RÉGI PAR L'ORDONNANCE N° 67.821 du 23.09.1967
Siège Social : Bd Henri Becquerel - 14000 CAEN (France) - R.C. Caen 997 888 300 C - Code APE 731Z - N° Siret 997 888 300 00016

High Precision Position Measurements at High Counting Rates with Drift Chambers and Multi-hit Electronics

M. Mac Cormick [a,1] W. Mittig [a] P. Roussel-Chomaz [a]
M.D. Cortina-Gil [a] C. Spitaels [a] J.F. Libin [a] J.M. Casandjian [a]
M. Chartier [a] F. Auger [b] S. Ottini [b] C. Mazur [c] Y. Blumenfeld [d]

[a] *GANIL, BP 5027, 14021 CAEN-Cedex, France*
[b] *CEA, DAPNIA/SPhN-CE Saclay, 91191 Gif-sur-Yvette Cedex, France*
[c] *CEA, DAPNIA/SED-CE Saclay, 91191 Gif-sur-Yvette Cedex, France*
[d] *Institut de Physique Nucléaire, IN2P3-CNRS, 91046 Orsay Cedex, France*

Abstract

High precision measurements of incident particle trajectories on an event-by-event basis is often an integral requirement of secondary beam experiments. Tests have been carried out using a system of low pressure drift chambers coupled to multi-hit TDC's. In this paper we report on the detection efficiency and "true" to "accidental" count rates measured for incident beam intensities ranging from 10^4 to 10^6 pps. It is demonstrated that the use of multi-hit TDC encoding allows the measurement of "true" and "accidental" coincidences in such a way that nearly 100% of the "true" events are recorded. The principal cause for the loss of a "true" event is due to the electronic dead time.

PACS numbers: 29.40.Cs, 29.40.Gx

1 Introduction

Many experiments using secondary beams require a high precision measurement of the incident particle trajectories on an event-by-event basis. At GANIL, heavy-ion secondary beams over a wide range of energies (~5 - 70 A.MeV),

nuclear charge (Z $\sim$ 1 - 50) and intensities ($\leq 10^6$ - 10^7 particles per second (pps)) are accessible.

The tests reported in this paper were carried out using the high resolution magnetic spectrometer SPEG [1]. The secondary beam, produced by fragmentation, is prepared with the aid of super-conducting solenoids (SISSI) [2] located at the exit of the second cyclotron. The beam is then transmitted to the SPEG experimental hall. In general, the beam is of poor quality, having a large emittance, ϵ. Normally, for standard high intensity primary beams, one may compensate for a large emittance by accepting only part of it; in this way the beam angular divergence and beam spot size may be controlled and adapted to the acceptance of SPEG.

The usual emittance used with SPEG for high resolution measurements is approximately 0.1 π mm mrad [3], as compared to the emittance of the secondary beams which is typically 16 π mm mrad. Cutting into the initial emittance leads to a significant loss in beam intensity. This solution is not practical as the secondary beam is, in general, already low in intensity. The alternative solution is to retain the full emittance, but this in turn leads to a loss in angular resolution.

To give an example, consider a primary beam at the monochromatic target point in SPEG. The beam spot on the target is typically $\pm$ 0.1 mm. The scattering angle, θ_{diff}, for a particle detected at the SPEG focal plane, $\theta_{focal\ plane}$, may be described as :-

$$\theta_{diff} = \theta_{focal\ plane} - \theta_{beam}$$

where θ_{beam} is the angle of the incident particle on the target. For this primary beam the angular divergence, $\Delta\theta_{beam}$, is $\sim \pm 0.3$ mrad. This divergence is lower than the typical experimental angular resolution of ± 0.5 mrad (at FWHM) and so the term θ_{beam} is negligable in the scattering angle calculation.

However, this is not the case for experiments that use secondary beams. In this case the nominal beam emittance is 16 π mm mrad and the beam spot size is typically $\sim \pm$ 1.5 mm. This results in a larger angular divergence of ± 3.4 mrad. In this case the beam divergence is greater than the angular resolution at the focal plane and so the term θ_{beam} can no longer be neglected. To obtain high resolution measurements with SPEG an angular divergence $\leq \pm 1$ mrad is neccessary. In order to match the beam angular divergence and the focal plane angular resolution the resolutions of θ_{beam} and $\theta_{focal\ plane}$ should be as similar as possible.

In this paper we present the results obtained for secondary beam tracking detectors that were developed at GANIL. Tests were carried out using a sys-

tem of low pressure drift chambers coupled to a multi-hit TDC. We give the detection efficiency, the "true" to "accidental" count rates for incident beam intensities ranging from 10^4 to 8×10^5 pps and the X, Y positional resolution. We show that the use of multi-hit TDC encoding allows the measurement of "true" and "accidental" coincidences in such a way that nearly 100% of the "true" events are recorded. The princical cause for the loss of a "true" event is due to the electronic dead time mask.

The beam tests were carried out at GANIL with a secondary beam produced by fragmentation of a ^{78}Kr primary beam at 73 A.MeV on a 100 mg/cm^2 Ni target. The position sensitive detectors were placed at the target point of SPEG. The incident beam particle's position was measured on an event-by-event basis.

2 The Drift Chambers

A single X, Y positional detector is comprised of 4 individual, similar drift chamber modules. One of the modules is shown schematically in figure i(a). Each module is filled with isobutane gas at 20 mbar. The isobutane is bubbled through isopropelyne alcohol at 4 °C to give a 1% mixture in the gas in order to slow down "ageing". The causes and effects of ageing have been widely studied by other groups and a detailed discussion with further references may be found in reference [4].

The anode-cathode voltage difference is -450 V and is evenly distributed throughout the drift region by equipotential strips deposited on the modules' entrance and exit windows. This provides a constant electric field of 3291 V cm^{-1} atm^{-1} within the drift region. The windows are made from 0.5 μm thick Mylar. A Frisch grid [5] at ground potential serves as the drift chamber anode as well as the partition that separates the drift region from the proportional counter. The electrons from the primary ionisation drift towards the proportional counter and are amplified around the proportional wire. It is the charge collected on this wire that is used in the position measurement. The drift velocity in the constant electric field is 5 cmμs^{-1}. The maximum drift time in the 70 mm drift region is therefore 1.4 μs.

To increase the signal to noise ratio (S/N), the pre-amplifiers are located as near as possible to the proportional read-out wires. The pre-amplifiers have a very high gain of 270 mV/MeV and are mounted directly on the detector support. The S/N, being optimised, means that we can work with a relatively low voltage on the proportional wire, which in turn, reduces the likelehood of ageing problems. The pre-amplifiers are in a hostile environment: they are in direct contact with the filling gas and are subjet to large current loads. Con-

sequently, several problems were encountered due to insufficient cooling. This led to some cross-talk problems which showed up as a negligable differential, non-linearity in the data.

The geometrical alignment of the detectors is such that the electric field in each module is orthogonal to the beam but the electron drift direction is different for each module. This is shown schematically in figure i(b). In this way two independent measurements of X (from modules X_{left} and X_{right} in figure i(b)) and Y (from modules Y_{up} and Y_{down}) are obtained. In section 5 we will discuss the analysis of this information.

3 Position Measurements

The principle of the position measurement is straightforward. The incident particles, on traversing the detector, ionise the gas within the drift chamber. These particles are then detected in a plastic scintillator (type NE102A), placed 14 m downstream from the detector, at the end of the SPEG focal plane. The scintillator is used as the triggering device and provides an external reference time which opens the multi-hit TDC gate (LeCroy 2277). This gate stays open during a pre-programmed 2 μs during which the delayed arrival of the electron drift times are recorded on the TDC input channels. The position of the incident particle is then deduced, and verified, from the recorded TDC times.

4 The Multi-hit TDC

The multi-hit TDC has 32 input channels and is used in the configuration where only one common start to the 32 channels is allowed for a given event. In the present experiment only four channels were used. Once the start is accepted an internal, programmable gate is generated during which all information on the input channels is digitized. A maximum of 16 data or "hits" per channel is allowed for a single event. Taking into account the maximum drift time of 1400 ns in the position detector, the internal gate was programmed to stay open for the slightly longer period of 2048 ns. The maximum time-out period programmable is 65 μs and is coded on 16 bits, giving a single bit time resolution of 1 ns. The double peak resolution is given as 5 ns peak to peak [6]. The data readout is zero compressed, thus giving rise to events of variable length.

5 Multi-hit Correlations

Events without at least one time recorded on each of the four input channels were rejected from all further analysis. These rejected events were used to caculate our detection efficiency (see section 8). For the remaining events, one must separate the "true" from the "accidental" coincidences.

We proceed by constructing a correlation diagram on which we plot all possible combinations of the times recorded, for example, for modules Y_{down} and Y_{up}. Such a plot is shown in figure ii for a pencil beam at 7×10^4 pps. On the same diagram we show the points obtained for a single event where times τ_{down}, τ'_{down} were recorded one TDC channel and times τ_{up}, τ'_{up} on another. We see that the point (τ_{down},τ_{up}) lies on the main correlation line, and therefore corresponds to the particle that triggered the plastic scintillator at time T_0. The combination $(\tau'_{down},\tau'_{up})$ lies on a weaker line, which lies parallel to the main correlation line, thus indicating that the TDC information is correlated and corresponds to the detection of a second particle in the drift chambers. However, with respect to the reference time, T_0, it is seen later than the line of "true" correlations. This is therefore an "accidental" coincidence. The other combinations (τ_{down},τ'_{up}) and (τ'_{down},τ_{up}) contain at least one of the "true" times but give uncorrelated pairs. They lie parallel to the axes τ_{down} and τ_{up}.

The length of the correlation line is proportional to the beam width and its width is a convolution of the velocity spread and the detector resolution. In figure iii, for the same pencil beam, we show (a) the sum and (b) the difference between the combinations, the latter gives us an image of the beam profile. We can see from this profile that the beam is offset from the center of the detector by a distance corresponding to a drift time of $\sim$110 ns. A second condition may now be applied to ensure that, as well as being correlated to the trigger, the particle lies within the beam profile. This effectively limits the acceptable length of the correlation line and is shown by the full vertical lines in figure iii(b).

These correlation diagrams are constructed for the pairs X_{left}, X_{right} and Y_{up}, Y_{down}. This gives two independent measurements of the incident particle's position, X and Y respectively.

6 Monte Carlo Simulations

A complete Monte Carlo simulation of the beam and detector configuration was carried out. This allowed a fuller understanding of the detector behaviour. The experimental parameters included in the simulation were divided into four

parts:-

- the beam characteristics;
- the beam impact point;
- the detector characteristics and
- the electronic characteristics

For the beam characteristics the parameters were comprised of the beam radio frequency (RF) at 12 MHz, the beam intensity, the FWHM of a single RF bunch and a Poisson distribution for the particle arrival times. The RF is such that we have one bunch every 83 ns, the TDC gate stays open for the pre-programmed 2048 ns, this means we are sensitive to roughly 24 beam bunches. The triggering particle has an average drift time of 700 ns during which time we may observe 7 bunches that preceed the triggering particle. Twenty four bunches were simulated for each event, the eighth systematically being chosen as the triggering particle. This simulates the time zone covered by the TDC gate.

The distribution of the beam impact points was chosen to resemble that of the experiment. In the Y dimension a Gaussian distribution with $\sigma = 0.31$ mm and an offset of 3.7 mm from the centre of the detector was appropriate. The wider spread X dimension was simulated by a flat distribution of 57.6 mm in width with an additional offset of 10 mm from the centre of the detector. In figure iv we show an example of the experimental results from which these conclusions were drawn.

The detector characteristics take into account the constant drift time for all particles, the theoretical arrival times may then be obtained. However the detector/electronic dead time mask of 200 ns allows the elimination of particles that arrive within 200 ns of each other. In the detector set-up the drift chamber signals were not sufficiently delayed, hence inducing a supplementary dead time of 187 ns after each trigger, as shown in figure iv(a). Recorded TDC times only in a limited range from 20 ns to 2040 ns were accepted for further study, both in the experimental and simulation analysis.

It is important to point out that the parameters used in the simulation allowed identical conditions to be applied to the basic parameters for both the experiment and the simulation. An excellent agreement between the simulated and experimental data was obtained. An example of a simulated beam is shown in figure v. The second particle type that can be seen in figure iv(a) was not simulated as its relative contribution is statistically negligable.

7 Comparative Study

The influences of the multi-hit capacity and the "length of the line" correlation method on the quality of the results were evaluated. In the following we discuss the results from the analysis of two configurations, namely :-

(i) Multi-hit TDC and correlations
(ii) Standard TAC (time-to-Analogue Convertor) with correlations

The success rate of finding a "true" event, insofar as it could be identified, with respect to the number of plastic triggers was evaluated. Both narrow beams and wide beams, of varying intensities, were considered.

Figure vi is a summary of the results from these analyses. In figure vi(a) the proportion of "true" events found in a multi-hit analysis using the correlation method (configuration (i) above) for a pencil beam is shown as a function of the incident beam count rate. The experimental results show a steady, linear decline, falling from 99% at $6{\cdot}7\times10^4$ pps to 83% at 8×10^5 pps. The simulation results for this analysis is shown in the same figure and are seen to be in good agreement with the experimental results. The same analysis with a wide beam is shown in figure vi(b) and follows the same behaviour as the pencil beam case and varies from 92% to 72%.

However, the success rate is systematically lower for the wider beam. A closer study of the simulated beam revealed two different effects that led to the loss of "true" events. The first, and main reason in this particular case, is the effect of the 187 ns trigger offset. As the beam is wide, particles fall near the edges of the detector and so one one the drift times may be shorter than the 187 ns offset. One of the "true" correlated times is then lost and only "accidental" combinations remain. The second reason occurs at higher intensities and is related to the beam geometry. The probability that two successive events may be in the detector at the same time for a given trigger is increased, as for the pencil beam case. However, assuming that the second particle provides the trigger, it may ionise the gas at the same position of the preceeding particle's drift electrons. In this way the "true" particle information will be lost. This scenario applies for all successive impact points that have a relative 200 ns drift time difference. The 200 ns is the dead time mask which clearly plays a more important role for wide beams at high intensities.

The results for configuration (ii), where a standard TAC measurement is employed for the position measurements are shown in figures vi(c) and (d). These results were obtained by analysis of the first hit on each channel for a given event. As expected, the success rate of finding a "true" correlated pair falls rapidly as the beam intensity increases. The values range from 97% to 61% for a pencil beam and 90% to 43% for a wide beam. Once again we see a good

agreement between the simulated and experimental data.

In order to quantify the advantage of using multi-hit electronics we take the difference between the multi-hit and standard TAC methods. This gives the gain in successfully finding a "true" solution relative to the standard approach. The experimental results are shown in figures vii(a) and (b) for a narrow and wide beam respectively. The corresponding simulated results are shown in figures vii(c) and (d) for completeness.

For these results we see a clear gain, rising from $\sim$2% at $6{\cdot}7\times10^4$ pps for both beam types to a maximum, at 8×10^5 pps, of 21% for a pencil beam and 29% for a wide beam.

8 Detection Efficiency

For a 100% efficient system we expect at least one time to be recorded on each of the TDC channels for every trigger. However, in practice this is not the case and so the detection efficiency is taken as being the ratio of the number of events where at least one time per channel is recorded to the number of triggers. In this particular case this results in a detection efficiency that is seen to be stable at $\sim$92% for all intensities. The main source of inefficiency is thought to arise from multiple scattering within the detector. No systematic study has been carried out to test the efficiency over a large range of particle masses and energies.

9 Spatial Resolution

The spatial resolution is found to be entirely independent of the beam count rate and is evaluted as being 0.3 mm for a pencil beam and 0.2 mm for a wide beam. This result is surprising as a degradation at higher intensities was expected. Due to the increased instantaneous charge in the detector, space-charge effects and pileup were expected. These effects surely play a more important role at higher intensities, but were evidently not important enough to degrade the resolution in the present study.

For two detectors placed at 1 m from each other then, without taking angular straggling into account, the expected angular resolution is $\sim$0.35 mrad in X and Y. However, this result is somewhat optimistic. In a recent experiment at GANIL a pair of these detectors were used for the initial angle reconstruction. An angular resolution of $\pm$0.5 mrad was evaluated. This higher value is due to the non-negligable angular straggling induced by the detectors. The result

is, however, entirely satisfactory as this resolution is of the same order as that of the focal plane detection system (± 0.5 mrad (FWHM)).

These detectors have been used successfully in several heavy-ion secondary beam experiments. They are reliable and simple to use and are now fully integrated into the "standard" SPEG detection system.

10 Conclusions

A system of high resolution position sensitive detectors, with a high rate counting capacity, has been successfully developed at GANIL. The resolution limit is imposed by angular straggling in the detectors, however, the spatial resolution is satisfactory for high resolution experiments. The use of multi-hit electronics provides a substantial gain in "true" event recording and "accidental" coincidences are easily identified by the correlation method. The main loss of information arises from the 200 ns dead time mask.

Figure Captions

(i) Schematical view of (a) the layout of a detector module, and (b) the complementary drift directions in each detector module.

(ii) A description of the correlation diagram for a pencil beam. The triggering particle is found in the zone labelled "correlated combinations and T_0", other correlated particles lie on the diagonal line and uncorrelated combinations lie parallel to the Y_{down} and Y_{up} axes. The structure of these lines arises from the beam radio frequency (RF) of 12 MHz.

(iii) For the same pencil beam as in figure ii, the cuts applied in the selection algorithm are shown as full vertical lines on either side of the peaks. Part (a) shows the "true" area taken from 1020 to 1125 ns for the acceptable "length of the line". Part (b) shows the beam profile. The accepted profile falls within the 30 to 230 ns zone.

(iv) (a) Some of the basic parameters taken fron the experiment and used in the simulation for a wide beam (at $1{\cdot}2\times10^5$ pps). The trigger offset, dead time and 2nd particle type are shown. The second particle type was not accepted in the analysis. (b) shows the "length of the line" and (c) shows the beam profile. The "true" events lie between the vertical lines drawn in (b) and (c).

(v) Simulated spectra for a wide beam at $1{\cdot}2\times10^5$ pps. (a) The correlation diagram, (b) the "length of the line" spectra and (c) the beam profile which may be compared with the experimental data in figures iv(a), (b) and (c).

(vi) The success rates of finding a "true" solution, as a percentage of the number of triggers, as a function of the incident beam count rate is shown. Each figure shows the experimental results (stars) as compared to the simulation results (crosses). Parts (a) and (b) show the results of multi-hit analyses for a pencil and wide beam respectively. Parts (c) and (d) show the results from a standard TAC approach.

(vii) The gain in successful particle tagging due to the use of a multi-hit TDC as compared to the standard TAC method is shown as a function of the incident beam intensity. Parts (a) and (b) show the experimental results for a pencil and wide beam respectively. Parts (c) and (d) show the equivalent results from the simulation analysis.

References

[1] L. Bianchi *et al.* ,
Nucl. Instr. Meth. **A276** (1989) 509.

[2] SISSI, Nuclear physics News,
Vol. 1, No.2, 1990, p.30

[3] A.C.C. Villari *et al.* ,
Nucl. Instr. Meth. **A281** (1989) 240-242.

[4] "Particle Detection with Drift Chambers"
W. Blum and L. Rolandi, Springer-Verlag, 1993.

[5] O. Frisch,
British Atomic Energy Report, BR-49 (1944)

[6] LeCroy, Operator's Manual,
Model 2277, 32 channel CAMAC TDC,
ECO 1004.

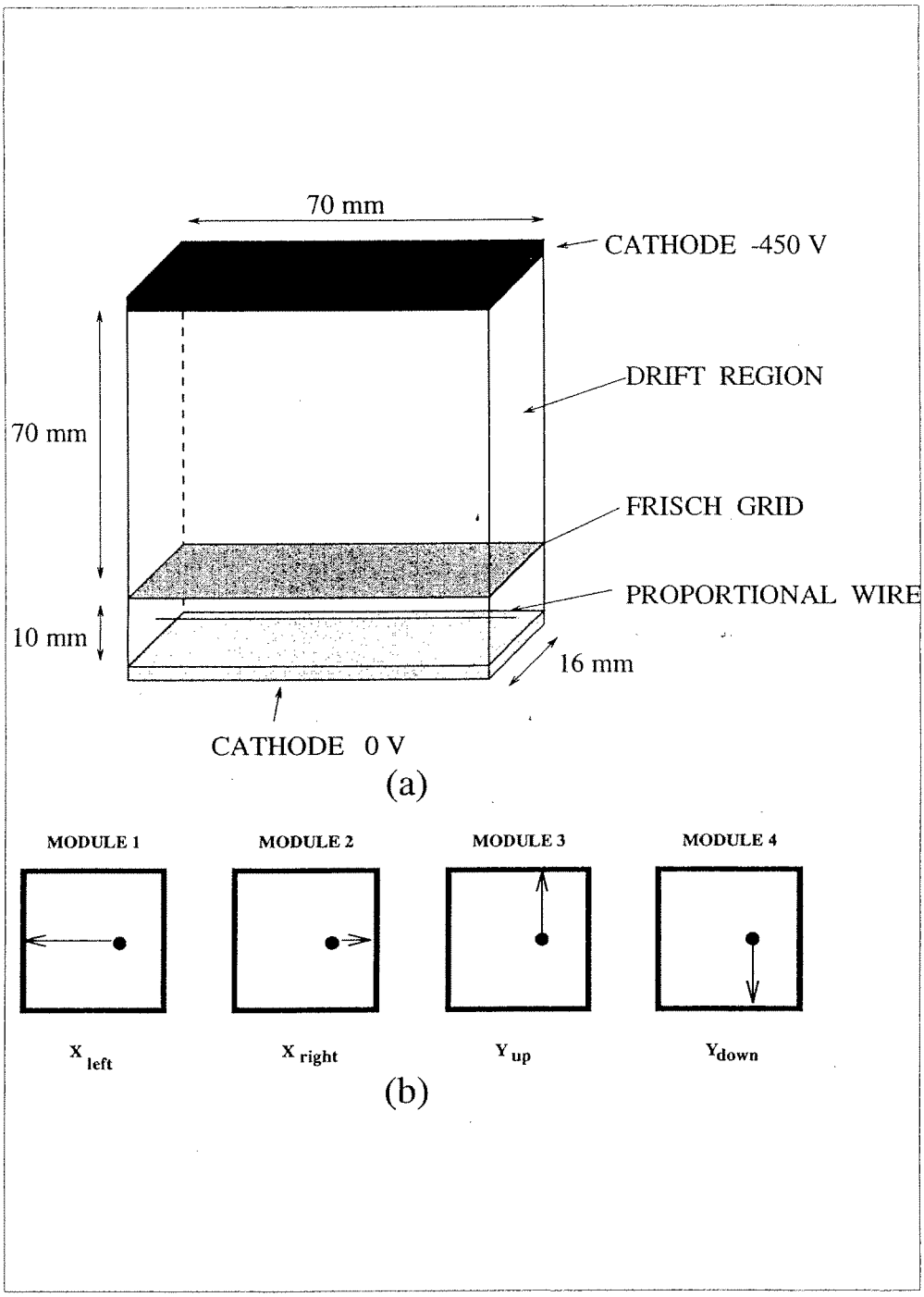
70 mm
CATHODE -450 V
DRIFT REGION
70 mm
FRISCH GRID
PROPORTIONAL WIRE
10 mm
16 mm
CATHODE 0 V
(a)
MODULE 1
MODULE 2
MODULE 3
MODULE 4
X left
X right
Y up
Y down
(b)

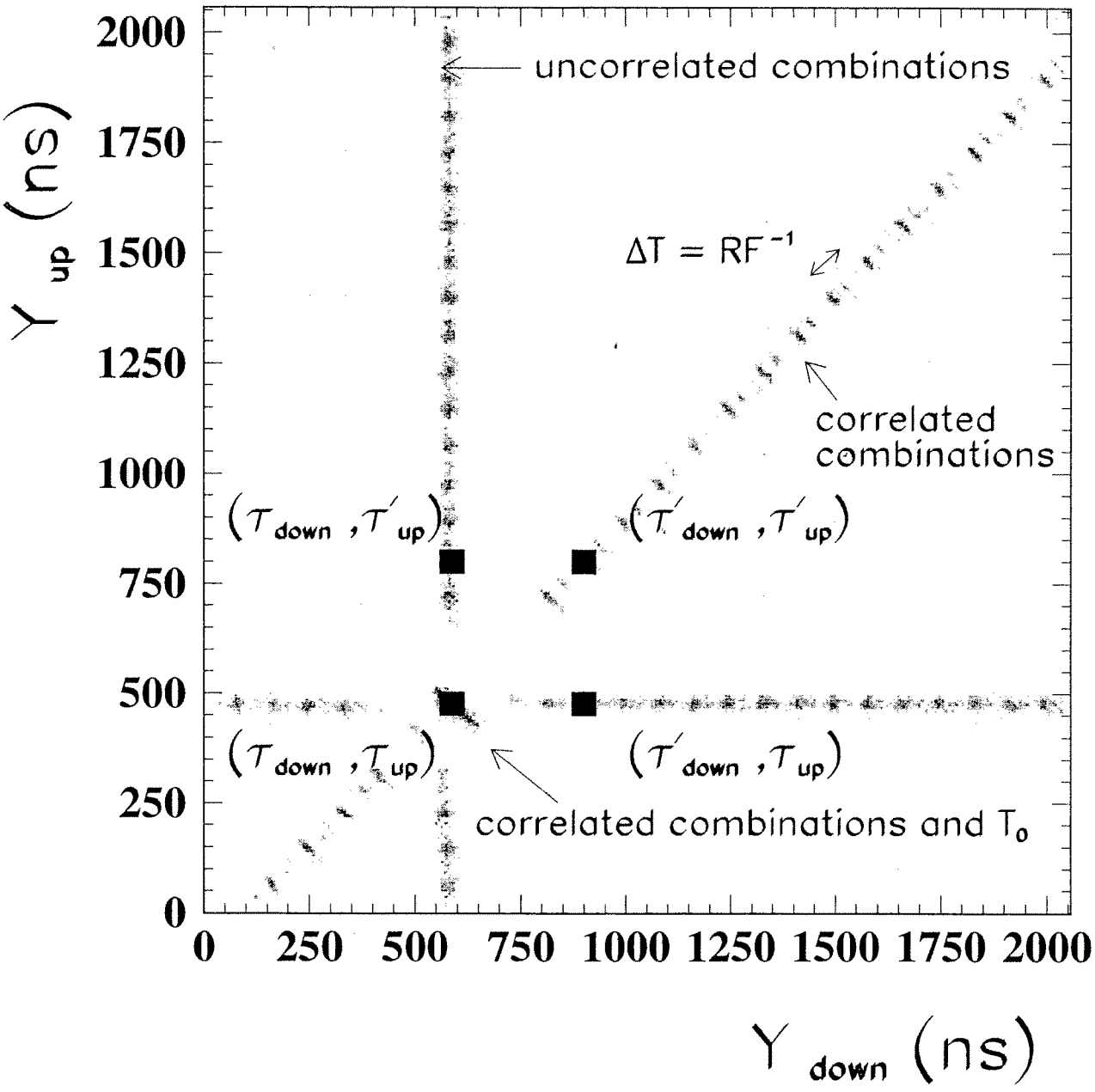
2000
1750
1500
1250
1000
750
500
250
0
0
250
500
750
1000
1250
1500
1750
2000
Y up (ns)
Y down (ns)
uncorrelated combinations
ΔT = RF⁻¹
correlated combinations
(τ down , τ' up)
(τ' down , τ' up)
(τ down , τ up)
(τ' down , τ up)
correlated combinations and T₀

Figure 2

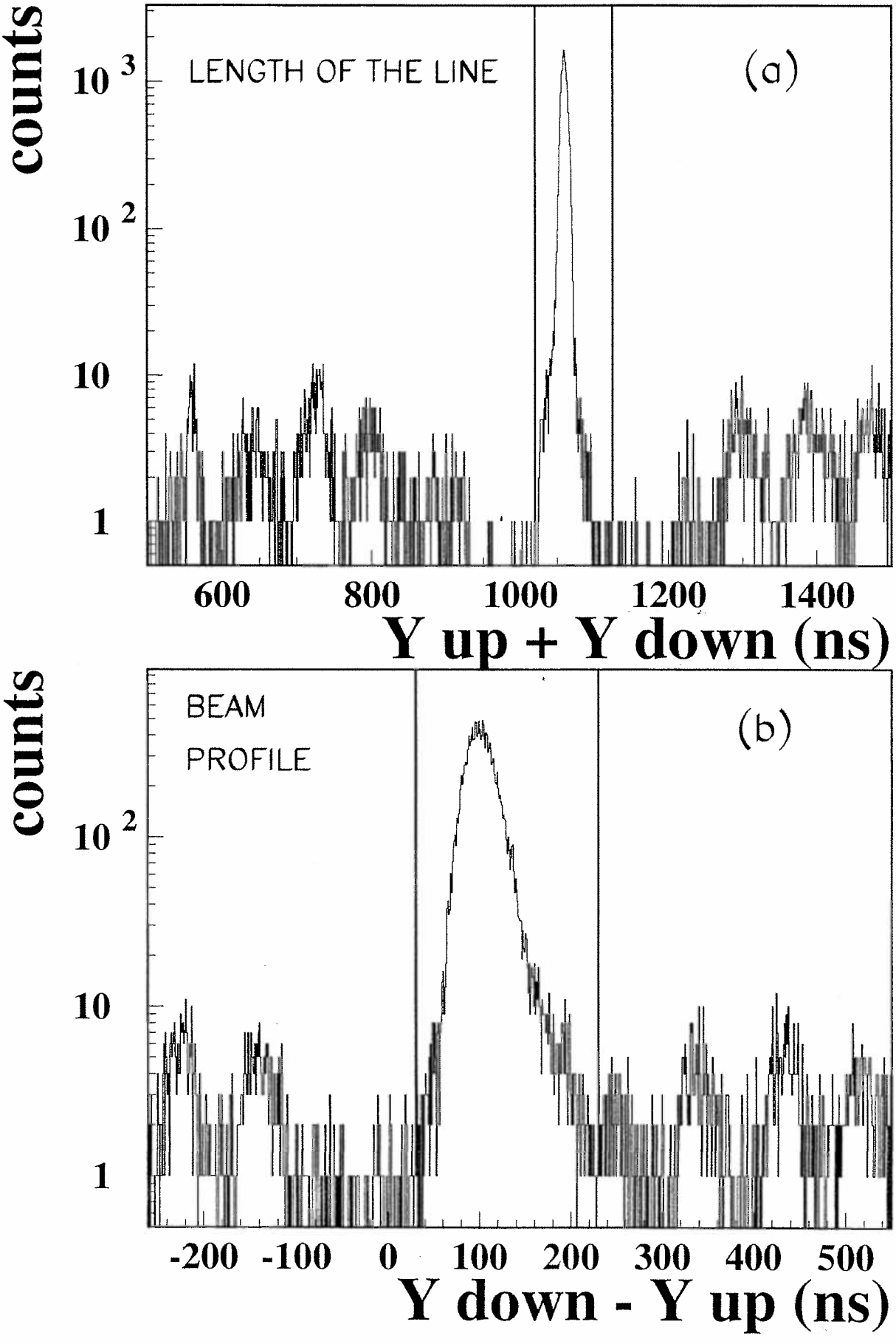
counts
LENGTH OF THE LINE
(a)
10 3
10 2
10
1
600
800
1000
1200
1400
Y up + Y down (ns)
counts
BEAM
PROFILE
(b)
10 2
10
1
-200
-100
0
100
200
300
400
500
Y down - Y up (ns)

Figure 3

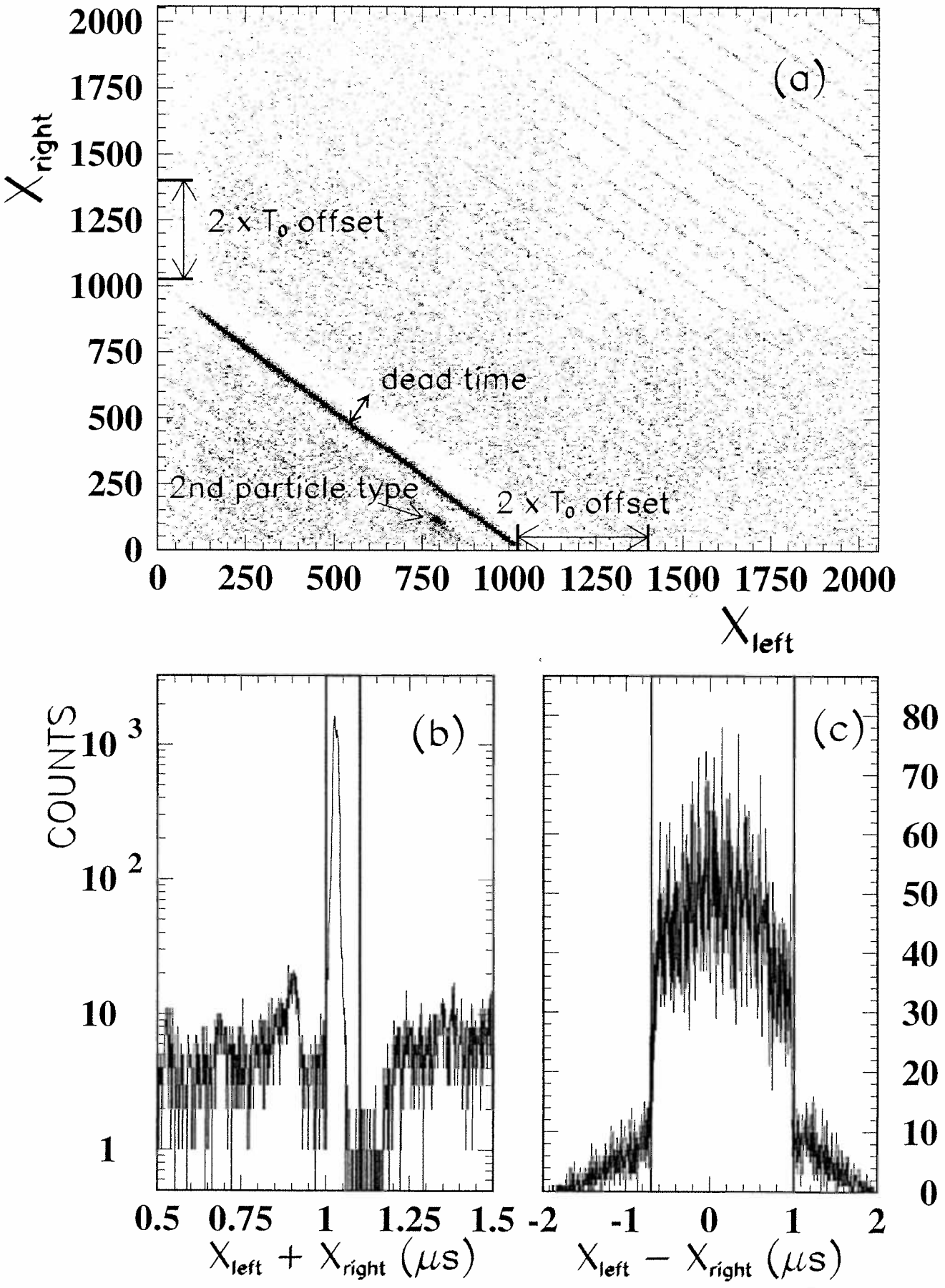
(a)
X_{right}
X_{left}
2 x T_o offset
dead time
2nd particle type
2 x T_o offset
0
250
500
750
1000
1250
1500
1750
2000
(b)
(c)
COUNTS
10^3
10^2
10
1
80
70
60
50
40
30
20
10
0
0.5
0.75
1
1.25
1.5
-2
-1
0
1
2
$X_{left} + X_{right}$ (μs)
$X_{left} - X_{right}$ (μs)

Figure 4

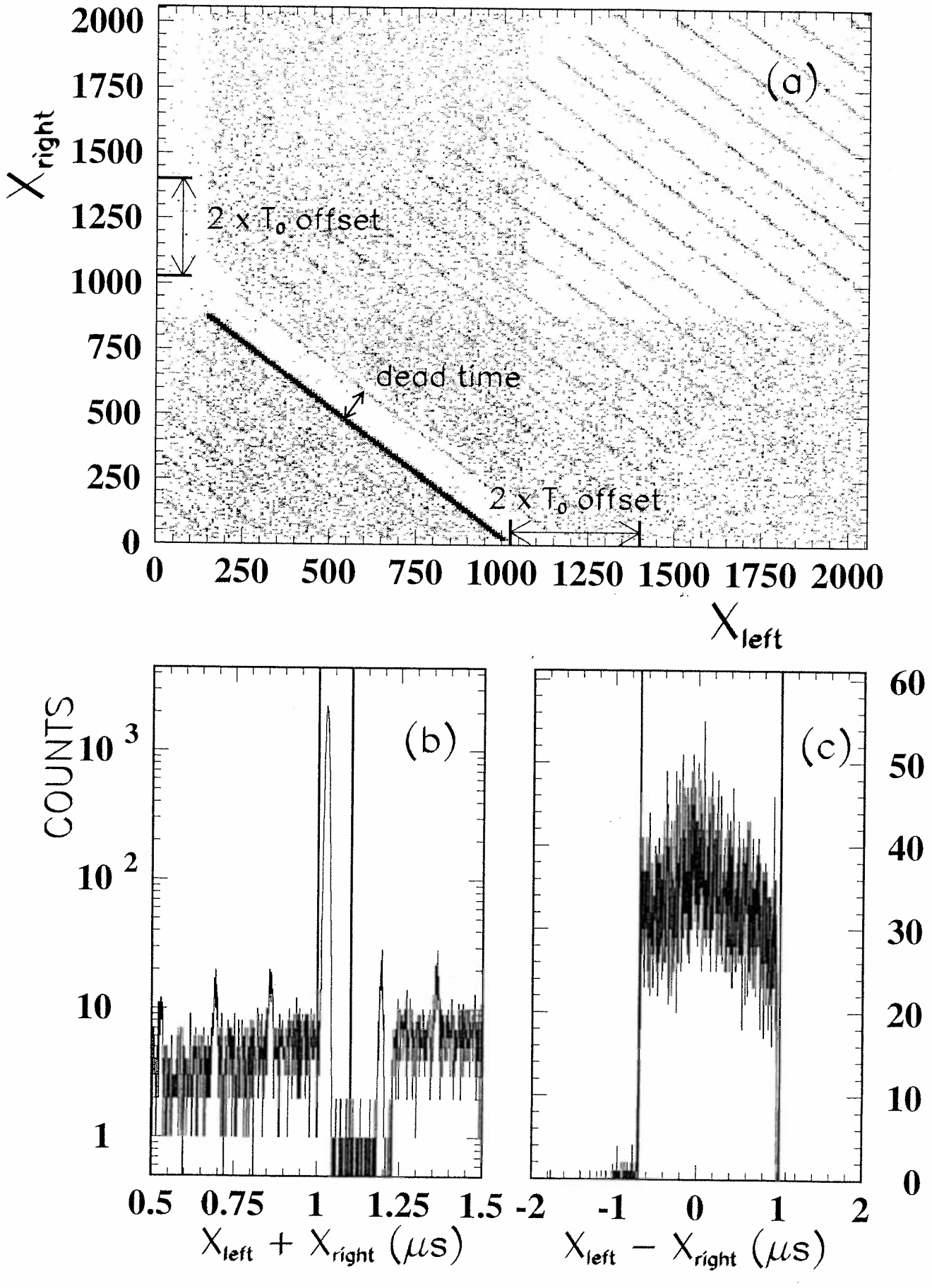
(a)
2 x T0 offset
dead time
2 x T0 offset
Xright
Xleft
2000
1750
1500
1250
1000
750
500
250
0
0 250 500 750 1000 1250 1500 1750 2000
(b)
(c)
COUNTS
10 3
10 2
10
1
0.5 0.75 1 1.25 1.5
-2 -1 0 1 2
60
50
40
30
20
10
0
Xleft + Xright (μs)
Xleft − Xright (μs)

Figure 5

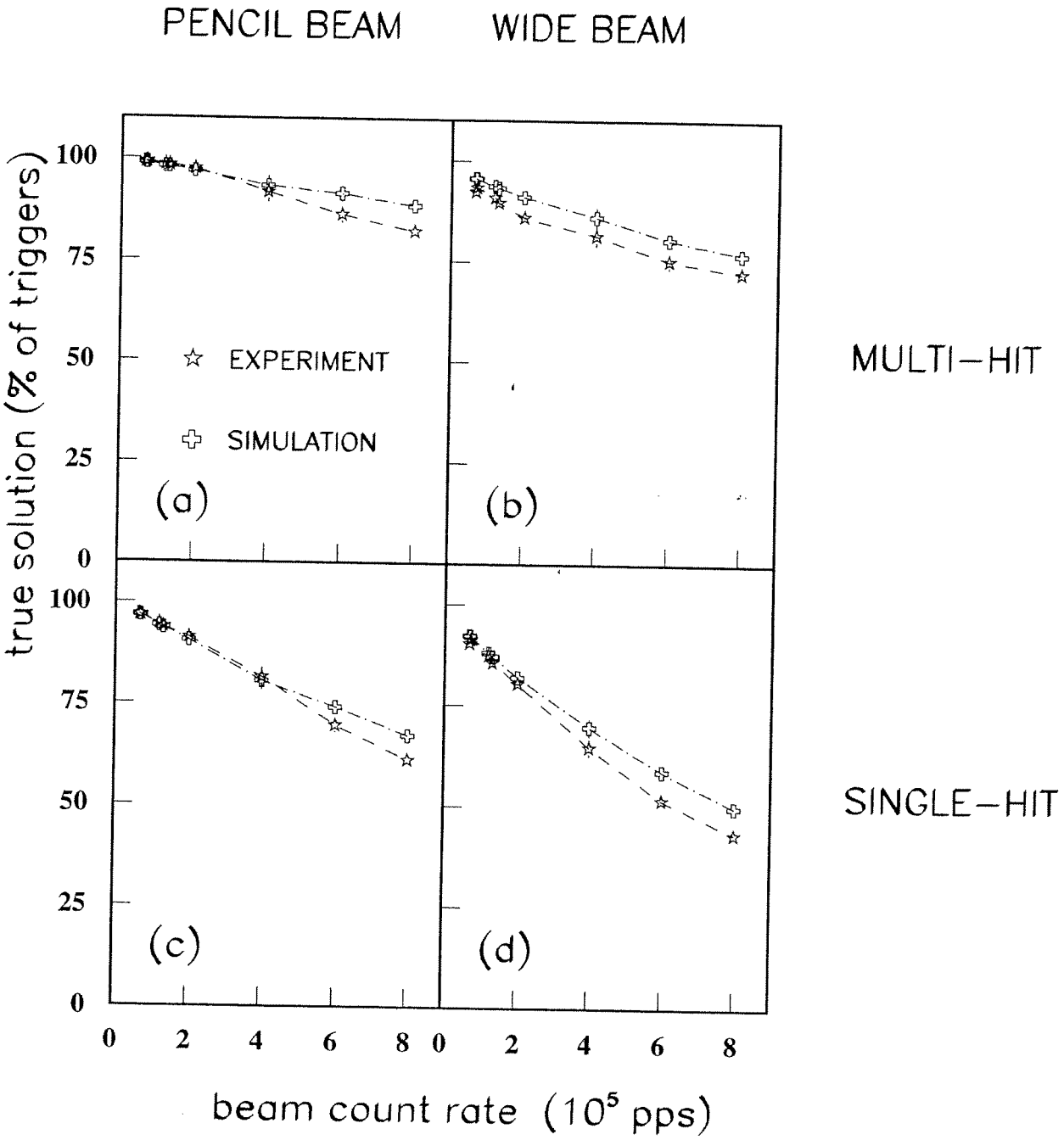
PENCIL BEAM
WIDE BEAM
MULTI–HIT
SINGLE–HIT
EXPERIMENT
SIMULATION
(a)
(b)
(c)
(d)
true solution (% of triggers)
beam count rate (10⁵ pps)
0
25
50
75
100
0
2
4
6
8

Figure 6

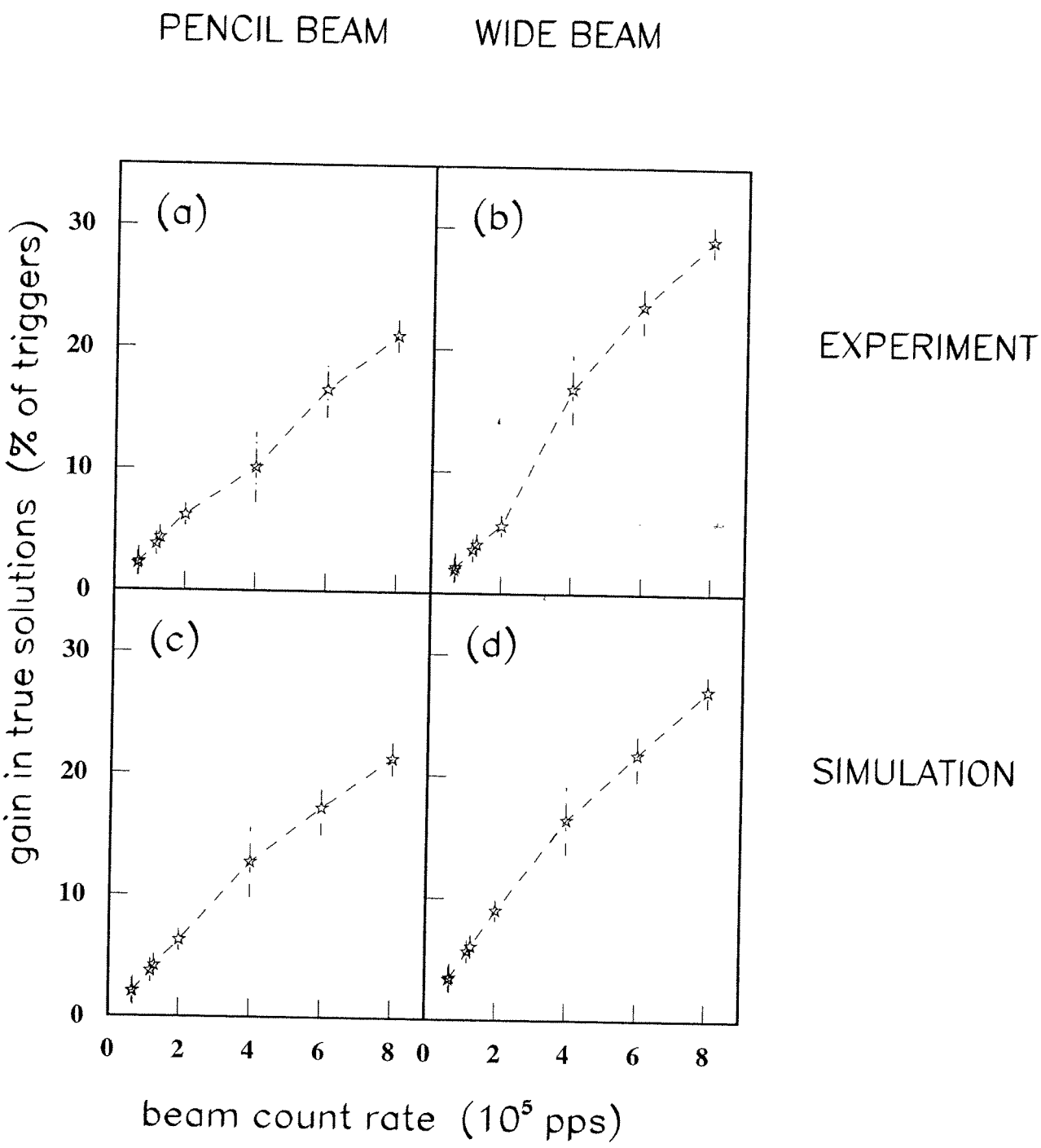
PENCIL BEAM
WIDE BEAM
(a)
(b)
(c)
(d)
EXPERIMENT
SIMULATION
gain in true solutions (% of triggers)
beam count rate (10^5 pps)
0
10
20
30
0
2
4
6
8

Figure 7